Accelerated Publications

Selectivity in Ligand Recognition of G-Quadruplex Loops†

Nancy H. Campbell, Manisha Patel, Amina B. Tofa, Ragina Ghosh, Gary N. Parkinson, and Stephen Neidle*

Cancer Research UK Biomolecular Structure Group, The School of Pharmacy, University of London, 29-39 Brunswick Square, London WC1N 1AX, U.K.

Received December 7, 2008; Revised Manuscript Received January 15, 2009

ABSTRACT: A series of disubstituted acridine ligands have been cocrystallized with a bimolecular DNA G-quadruplex. The ligands have a range of cyclic amino end groups of varying size. The crystal structures show that the diagonal loop in this quadruplex results in a large cavity for these groups, in contrast to the steric constraints imposed by propeller loops in human telomeric quadruplexes. We conclude that the nature of the loop has a significant influence on ligand selectivity for particular quadruplex folds.

Nucleic acid sequences containing short tracts of guanine residues can form higher-order quadruplex structures (*1, 2*). Quadruplexes can be intramolecular, with four or more G-tracts, or intermolecular, with one or two G-tracts. They have been extensively investigated by structural and biophysical methods, and a number of distinct topologies have been found. They depend in large part on the sequence and size of the intervening loops. Chain-reversal (propeller) loops are positioned on the exterior of quadruplex structures, whereas diagonal and edge (lateral) loops are stacked onto the terminal G-quartets of a quadruplex structure.

Two principal categories of quadruplex nucleic acids have received attention as potential therapeutic targets: (i) those capable of being formed at the single-stranded overhang of telomeric DNA, for which appropriate small-molecule ligands can induce quadruplex formation, inhibit the activity of the telomerase enzyme complex, and selectively target telomere maintenance in cancer cells (*3, 4*), and (ii) those within genomes (*5, 6*) and especially within promoter sequences of genes involved in cellular proliferation (*7*) such as vascular endothelial growth factor (*8, 9*), and oncogenes such as *c-myc* (*10*−*14*) and *c-kit* (*15*−*18*). It has been suggested (*9, 10*) that ligands selective for promoter quadruplexes could in principle downregulate the expression of these genes and thus have an anticancer effect.

A wide range of small molecules have been investigated as quadruplex-binding and -stabilizing ligands (see recent reviews in refs *19* and *20*). The majority share the common structural features of (i) a planar heteroaromatic chromophore, which stacks by $\pi-\pi$ interactions onto the G-quartet motif at the terminus of a quadruplex, and (ii) short alkyl chain substituents normally terminating in an amino group that is fully cationic at physiological pH. The precise nature of these substituents has been found to influence quadruplex affinity and selectivity. For example, the size of the terminal amino substituent has a major influence on the affinity and energetics of substituted acridine binding to a human intramolecular telomeric DNA quadruplex (*21*). The nature of the substituent together with side chain length has been rationalized for series of trisubstituted acridine ligands (having 3-pyrrolopropionamido chains at the 3- and 6-positions) (*22, 23*) on the basis of a cocrystal structure with a human telomeric DNA quadruplex (*24*). The propeller loops on the exterior of this quadruplex change their conformation from those found in the native structure (*25*) to form discrete binding pockets for the substituents. By contrast, the bimolecular quadruplex from the organism *Oxytricha nova* has a diagonal loop of sequence d(TTTT) stacked on top of the quadruplex (*26*). A cocrystal structure with an acridine derivative disubstituted with the same 3-pyrrolopropionamido group (Figure 1, compound **7**) shows this ligand bound between the loop and a terminal G-quartet (*27*). Structural

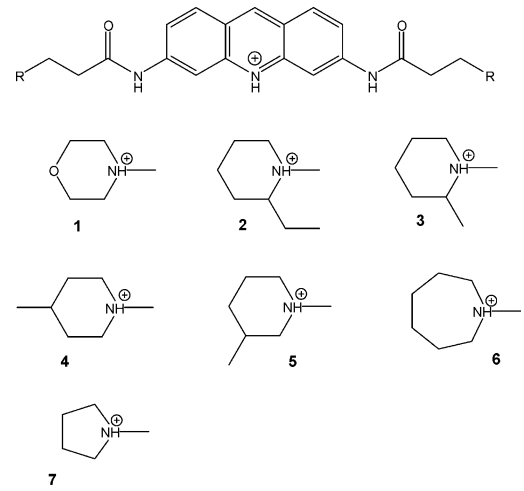

FIGURE 1: Structures of 3,6-disubstituted acridines in this study.

† This work was supported by CRUK and the EU (FP6 Project on Molecular Cancer Medicine).

* To whom correspondence should be addressed. Phone: +44 (0)20 7753 5971. Fax: +44 (0)20 7753 5970. E-mail: stephen.neidle@pharmacy.ac.uk.

10.1021/bi802233v CCC: $40.75
Published on Web 01/27/2009

Table 1: Crystallographic Details of the Quadruplex−Acridine Complexes That Are Reported in This Study[a]

	1	2a	2b	3	4	5	6
PDB entry	3EM2	3EQW	3EUI	3ERU	3ES0	3ET8	3EUM
cell dimensions [*a*, *b*, *c* (Å)]	55.23, 42.71, 26.84	55.28, 42.73, 26.62	55.36, 42.54, 48.64	55.22, 42.63, 26.85	55.53, 42.46, 27.30	55.40, 42.59, 27.14	55.62, 42.31, 27.08
space group	$P2_12_12$	$P2_12_12$	$P2_12_12_1$	$P2_12_12$	$P2_12_12$	$P2_12_12$	$P2_12_12$
resolution (Å)	2.30	2.20	2.20	2.00	2.20	2.45	1.78
no. of observed reflections	3000	3454	5575	4422	3549	2602	5372
% observed reflections	97.0	99.6	94.5	95.7	99.7	99.7	81.7
R	0.20	22.6	23.4	20.1	19.7	21.1	22.4
R_{free}	0.29	31.4	28.5	24.9	24.5	27.7	27.0
R_{merge}	0.057	0.092	0.087	0.059	0.041	0.084	0.079
$\langle B \rangle$ (Å^2)	17.0	12.9	20.7	17.4	11.1	16.6	16.5
no. of observed water molecules	64	66	159	71	56	51	52

[a] Further information is available in the individual PDB entry.

information about quadruplex−ligand complexes is limited to a small number of NMR-derived (*13, 28, 29*) and crystal structures (*24, 27, 30, 31*), and as yet, it has not been possible to define the structural features that differentiate small molecule binding to one quadruplex compared to another. Evidence is accumulating that it is possible to target particular quadruplex types, as shown by the binding of diarylethynyl amides to a parallel topology formed by a quadruplex formed by a sequence within the *c-kit* promoter (*32*).

This study addresses the issue of ligand selectivity by examining how ligand binding is constrained by loop geometry in two distinct quadruplex architectures. The *O. nova* bimolecular quadruplex has been used as an exemplar for one particular type of loop, the diagonal type, formed in this instance by four thymine nucleotides. We report here on six cocrystal structures of disubstituted acridines with this quadruplex (Figure 1), to examine how the T_4 diagonal loop accommodates differences in substituent size in a range of closely related compounds (ligands **1**−**7**). The results are compared to the geometry observed with the trisubstituted acridine compound BRACO-19 bound to the human bimolecular quadruplex that has purely propeller loops (*24*).

MATERIALS AND METHODS

General. The synthesis of the disubstituted acridines has been previously described (*33*). All compounds were analytically pure and were used as the hydrochloride salts, apart from compound **1**, which was used as the free base. The oligonucleotide d(GGGGTTTTGGGG) was purchased from Eugentec and HPLC-purified by them. It was annealed at 90 °C prior to use.

Crystallography. All crystals were obtained at 12 °C by the hanging-drop vapor-diffusion method. Typical conditions were 2 μL drops containing 5% (v/v) methyl-2,4-pentanediol (MPD), 0.50 mM oligonucleotide, 0.25 mM ligand, 40 mM KCl, 5 mM $MgCl_2$, and 4.1 mM spermine equilibrated against 35% (v/v) MPD, at pH 7.0.

Crystallographic data for all except one structure were collected on an in-house Rigaku R-AXIS-IV image plate system with a rotating-anode source using Osmic mirror optics to produce monochromatic Cu Kα radiation at a wavelength of 1.54178 Å. Data for Protein Data Bank (PDB) entry 3EUM (ligand **6**) were collected on an Oxford Diffraction Nova system equipped with a ccd detector and a sealed tube/microfocus system. All crystals were flash-frozen using glycerol cryoprotectant and were maintained at 105 K during data collection. Unit cell parameters and data collection information are given in Table 1. Processing and data reduction were carried out using the DTREK part of the Crystal Clear software package (Rigaku Inc.) for all data sets apart from that for ligand **7**, which was processed with Crysalis (Oxford Diffraction).

Structures were determined by molecular replacement using PHASER (*34*) from the CCP4 package (*35*) and the known acridine−*Oxytricha* structure (*27*) as a starting point. In each case, the top solution was the one that satisfactorily refined and, for all the structures apart from that with the larger unit cell, was in the same position in the cell as determined previously in the complex with compound **7** (*27*). Electron density and difference maps were used to define the ligand structure and locate solvent molecules. All structures were refined in the same manner using the CCP4 package (*35*) and REFMAC (*36*). Crystallographic data are given in Table 1. All structures have been deposited in the Protein Data Bank with both coordinates and structure factors being available.

RESULTS AND DISCUSSION

A total of six ligands were cocrystallized with the *Oxytricha* telomeric DNA sequence d($G_4T_4G_4$) and form bimolecular quadruplex crystal structures isomorphous with the native structure (PDB entries 1JPQ and 1JRN) (*26*) and the previously reported complex with compound **7**, in space group $P2_12_12$ (PDB entry 1L1H) (*27*). Crystals of a second form with compound **2** were also obtained, having two independent quadruplex complexes in the asymmetric unit. These two structures are closely similar to the other complexes.

All structures (Table 2) have the acridine compounds bound in a manner identical to that previously found (*27*) for compound **7** (Figure 2), with one ligand bound per bimolecular quadruplex, and stacked between a terminal G-quartet of the quadruplex and thymine bases from the T_4 loop. The acridine chromophore forms a pair of hydrogen bonds in all the structures with a loop thymine base that is in the same plane as the acridine (Table 2 and Figure 2). The formation of a hydrogen bond between thymine O2 and the central ring nitrogen atom of the acridine [with a mean distance of 3.0(1) Å in all the complexes] suggests that this nitrogen atom is protonated. A similar arrangement has been

Table 2: Selected Ligand−Thymine Intermolecular Distances (angstroms) and Side Chain Torsion Angles (deg)[a]

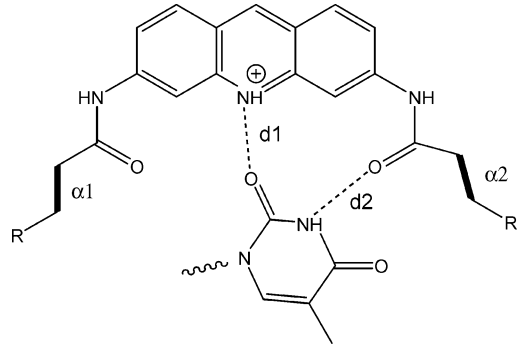

	1	2a	2b	3	4	5	6	7	BRACO-19
PDB entry	3EM2	3EQW	3EUI	3ERU	3ES0	3ET8	3EUM	1L1H	3CE5
d_1	3.1	3.1	3.1, 2.9	2.9	3.0	2.9	2.9	3.0	NA
d_2	2.7	2.7	2.8, 2.8	2.8	2.7	2.7	2.7	2.7	NA
α_1	238	230	225, 215	230	232	243	238	160	217
α_2	180	161	153, 145	175	112	187	180	212	172

[a] Structure 3EUI has two quadruplex−ligand complexes in the asymmetric unit. Structure 3CE5 has water-mediated hydrogen bonds between the thymine ring and the acridine group, so distances d_1 and d_2 are not directly comparable.

observed in the telomeric BRACO-19 acridine quadruplex complex (*24*), but with a water molecule bridging by hydrogen bonds the central ring of the acridine and the thymine ring. Structural changes in the *Oxytricha* quadruplex itself are minimal between all the ligand−complex crystal structures and the native structure, and the overall root-mean-square (rsmd) is <0.2 Å for all structures. Amide and side chain conformations in the acridine derivatives and first-shell water environments are also unchanged in all the structures.

The morpholino groups in compound **1** are expected to be neutral at physiological pH, whereas the ring nitrogen atom in all the other compounds should be protonated. This difference is reflected in the consistent findings of superior quadruplex binding and biological responses of acridine-based and many quadruplex-binding ligands that have cationic charged side chains (*19*−*23*). It is notable that there are no direct amine nitrogen−phosphate contacts in any of these structures or any indirect amine−water−phosphate bridges, which have been observed in the BRACO-19 complex crystal structure (*24*). We cannot exclude the possibility that some water molecules in the vicinity of the amine groups in these diacridine structures have not been observed due to increased water mobility or the resolution limits of the data. Otherwise, it is suggested that the charged amine groups in compounds **1**−**7** exert their effect on ligand binding through long-range electrostatic interactions. Alternative end groups with an amine nitrogen atom next to the side chain would bring the charged nitrogen closer to a phosphate group; such analogues do not appear to have been investigated to date.

The conformations of the cyclic amine end groups and side chains of the acridine ligands all cluster together (Figure 3), although the methyl groups attached to the piperidino rings are oriented in a variety of directions (Table 2). This confirms what can be observed visually, that there is a significant volume of space that is accessible to all the rings and their substituents. The para methyl compound **4** has its substituted piperidino ring flipped into a region with a larger volume that can accommodate its para substitution, as shown by the difference of ca. 60° in side chain torsion angle α_2. Both ortho ethyl substituents in compound **2** are relatively close to backbone and sugar oxygen atoms, suggesting that a suitable ortho substituent such as a methylene hydroxyl group could form additional hydrogen bonds to O3′ or phosphate oxygen atoms.

The regions in the telomeric quadruplex acridine complex (*24*) around the BRACO-19 ligand have some resemblance to those around the disubstituted acridines. In both cases, the in-plane thymine originates from a loop, but whereas the thymines require only minimal conformational change compared with the native state to achieve this since the diagonal loop is already in place over the binding site, the parallel loop has to undergo a more profound change to place the thymine in-plane. This and changes in the other parallel loop in the telomeric structure result in the formation of discrete binding pockets that are bounded by phosphate groups from the loops and accommodate the pyrrolidino rings at the end of the BRACO-19 side chains (Figure 4a). Acridine compounds with larger ring substituents have reduced quadruplex affinity; a piperidino ring results in a 7-fold lower K_a, and an eight-membered ring gives a further 3-fold reduction (*21*). By contrast, the results presented here show that the binding site beneath the diagonal loop in the *Oxytricha* quadruplex is able to accommodate, without any distortion, a piperidino ring, even when it has methyl or ethyl substituents, as well as a seven-membered ring. An eight-membered ring has been modeled into an *Oxytricha* binding site (Figure 4b), and this similarly does not produce any structural perturbations; it is too bulky to fit into the telomeric quadruplex pocket.

We ascribe these differences to the distinct disposition of the loops in these structures: the external placement of propeller loops will affect substituent groups attached to a chromophore, whereas the bases in four-nucleotide diagonal loops are involved in $\pi-\pi$ stacking with the chromophore itself. Thus, in broad terms, a diagonal loop allows considerable latitude in the length and size of substituents, whereas the presence of a propeller loop would impose severe constraints on substituents. The overall volume of the

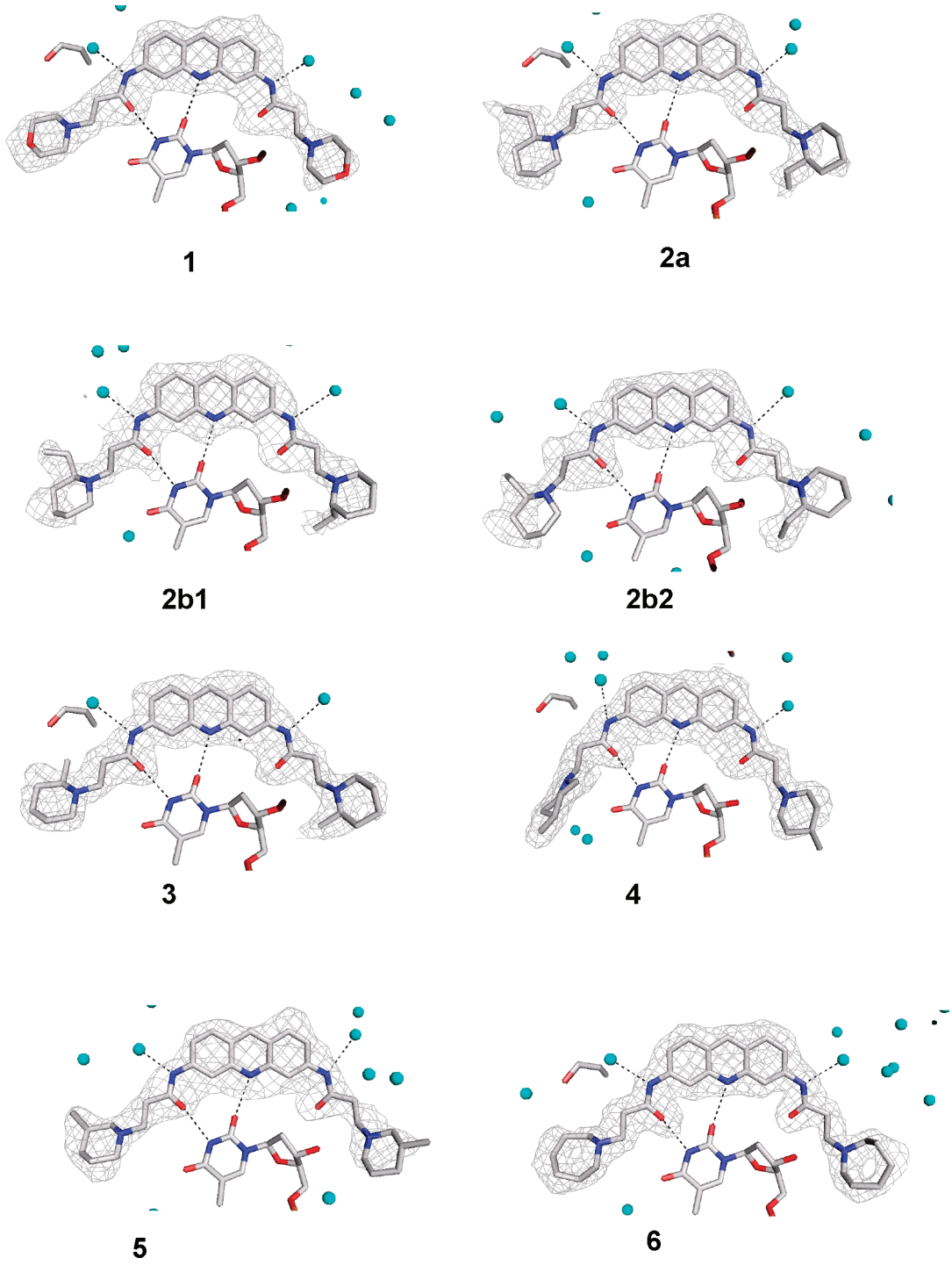

FIGURE 2: Omit map views of the crystal structures, looking onto the acridine plane. In each case, the thymine hydrogen bonding to the acridine chromophore is shown. Electron density is drawn at a 1.5σ level.

overlaid end group rings, taken together, is 66 Å^3 greater than that of the piperidino rings of BRACO-19 in its complex, and the surface area is 54 Å^2 greater. Examination of the *Oxytricha* structures indicates that there is no steric barrier to an individual end group being larger than suggested by this total overlaid volume.

The exact length and sequence of a propeller loop will define the size and surface charge characteristics of the pocket that it can form. Since these loops are formed by short ≤3-nucleotide sequences (*37*−*39*), it is likely that there will be similar steric constraints on the size of ligand substituents for binding to all quadruplexes that contain propeller loops (for example, refs *8*, *9*, *12*, *17*, *25*, and *40*−*45*). Structural studies have suggested that diagonal loops may be rather less prevalent among human genomic quadruplexes, although one is present in the quadruplex formed by the five guanine tracts in the *c-myc* promoter (*13*), with the porphyrin TMPyP4 ligand bound in the loop environment. The porphyrin substituent groups in this structure are fully exposed, analogous to the end groups in the structures presented here.

We suggest that the principle of loops constraining side chain substitution should be useful in the future design of small molecules targeting individual quadruplexes, when

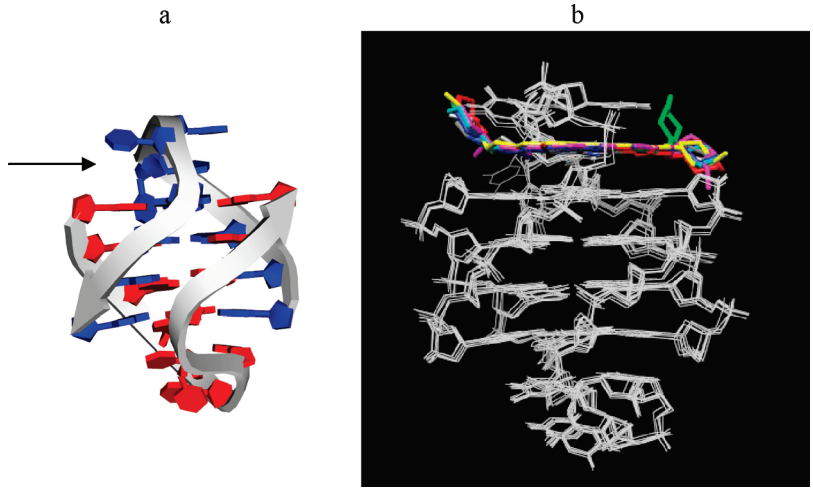

FIGURE 3: (a) Cartoon representation of the bimolecular *O. nova* quadruplex, drawn using crystallographic coordinates of structur 33EUM. The bases of one individual d(GGGGTTTTGGGG) molecule are colored red, and the second is colored blue. The view of the molecule is the same as in panel b. The ligand binding site is indicated by an arrow. (b) Overlay of the quadruplex complexes in all eight disubstituted acridine crystal structures. The quadruplexes are shown in white wireframe form, and the ligands are shown in color stick representation: compound **1** in blue, compound **2** in mauve, compound **3** in cyan, compound **4** in green, compound **5** in yellow, compound **6** in red, and compound **7** in gray.

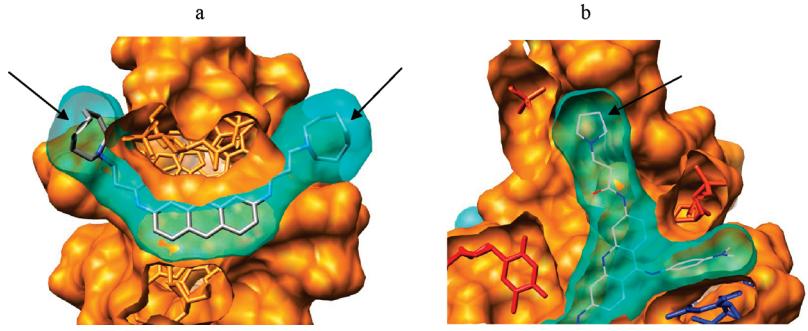

FIGURE 4: (a) Structure of the *O. nova* quadruplex complex with compound **6**, which has been modified and energy-minimized to have terminal eight-membered rings (indicated by arrows). Note the open nature of the regions where these rings reside. (b) Solvent-accessible surface of the acridine−human telomeric quadruplex structure (*24*), showing the acridine in cyan and the close packing between the surfaces of the terminal pyrrolidino ring (indicated by an arrow) and the pocket formed by the TTA parallel loop.

there is prior knowledge of overall quadruplex topology and therefore of the nature of the loops. Further insights into how ligand substituents impart selectivity for a particular quadruplex must await additions to the number of detailed quadruplex three-dimensional structures.

ACKNOWLEDGMENT

We are grateful to Oxford Diffraction Ltd. and Dr. Marcus Winter for granting us time on their facilities.

REFERENCES

1. Burge, S. E., Parkinson, G. N., Hazel, P., Todd, A. K., and Neidle, S. (2006) Quadruplex DNA: Sequence, topology and structure. *Nucleic Acids Res. 34*, 5402–5415.
2. Patel, D. J., Phan, A. T., and Kuryavyi, V. (2007) Human telomere, oncogenic promoter and 5′-UTR G-quadruplexes: Diverse higher order DNA and RNA targets for cancer therapeutics. *Nucleic Acids Res. 35*, 7429–7455.
3. Oganesian, L., and Bryan, T. M. (2007) Physiological relevance of telomeric G-quadruplex formation: A potential drug target. *BioEssays 29*, 155–165.
4. de Cian, A., Lacroix, L., Douarre, C., Temime-Smaali, N., Trentesaux, C., Riou, J.-F., and Mergny, J.-L. (2008) Targeting telomeres and telomerase. *Biochimie 90*, 131–155.
5. Huppert, J. L., and Balasubramanian, S. (2005) Prevalence of quadruplexes in the human genome. *Nucleic Acids Res. 33*, 2908–2916.
6. Todd, A. K., Johnston, M., and Neidle, S. (2005) Highly prevalent putative quadruplex sequence motifs in human DNA. *Nucleic Acids Res. 33*, 2901–2907.
7. Huppert, J. L., and Balasubramanian, S. (2007) G-quadruplexes in promoters throughout the human genome. *Nucleic Acids Res. 35*, 406–413.
8. Guo, K., Gokhale, V., Hurley, L. H., and Sun, D. (2008) Intramolecularly folded G-quadruplex and i-motif structures in the proximal promoter of the vascular endothelial growth factor gene. *Nucleic Acids Res. 36*, 4598–4608.
9. Sun, D., Liu, W. J., Guo, K., Rusche, J. J., Ebbinghaus, S., Gokhale, V., and Hurley, L. H. (2008) The proximal promoter region of the human vascular endothelial growth factor gene has a G-quadruplex structure that can be targeted by G-quadruplex-interactive agents. *Mol. Cancer Ther. 7*, 880–889.
10. Siddiqui-Jain, A., Grand, C. L., Bearss, D. J., and Hurley, L. H. (2002) Direct evidence for a G-quadruplex in a promoter region and its targeting with a small molecule to repress c-*MYC* transcription. *Proc. Natl. Acad. Sci. U.S.A. 99*, 11593–11598.
11. Hurley, L. H., Von Hoff, D. D., Siddiqui-Jain, A., and Yang, D. (2006) Drug targeting of the c-MYC promoter to repress gene expression via a G-quadruplex silencer element. *Semin. Oncol. 33*, 498–512.
12. Phan, A. T., Modi, Y. S., and Patel, D. J. (2004) Propeller-type parallel-stranded G-quadruplexes in the human c-myc promoter. *J. Am. Chem. Soc. 126*, 8710–8716.
13. Phan, A. T., Kuryavyi, V., Gaw, H. Y., and Patel, D. J. (2005) Small-molecule interaction with a five-guanine-tract G-quadruplex structure from the human MYC promoter. *Nat. Chem. Biol. 1*, 167–173.

14. Ambrus, A., Chen, D., Dai, J., Jones, R. A., and Yang, D. (2005) Solution structure of the biologically relevant G-quadruplex element in the human c-MYC promoter. Implications for G-quadruplex stabilization. *Biochemistry 44*, 2048–2058.
15. Rankin, S., Reszka, A. P., Huppert, J., Zloh, M., Parkinson, G. N., Todd, A. K., Ladame, S., Balasubramanian, S., and Neidle, S. (2005) Putative DNA quadruplex formation within the human c-kit oncogene. *J. Am. Chem. Soc. 127*, 10584–10589.
16. Fernando, H., Reszka, A. P., Huppert, J., Ladame, S., Rankin, S., Venkitaraman, A. R., Neidle, S., and Balasubramanian, S. (2006) A conserved quadruplex motif located in a transcription activation site of the human c-kit oncogene. *Biochemistry 45*, 7854–7860.
17. Phan, A. T., Kuryavyi, V., Burge, S., Neidle, S., and Patel, D. J. (2007) Structure of an unprecedented G-quadruplex scaffold in the human c-kit promoter. *J. Am. Chem. Soc. 129*, 4386–4392.
18. Todd, A. K., Haider, S. M., Parkinson, G. N., and Neidle, S. (2007) Sequence occurrence and structural uniqueness of a G-quadruplex in the human c-kit promoter. *Nucleic Acids Res. 35*, 5799–5808.
19. Monchaud, D., and Teulade-Fichou, M. P. (2008) A hitchhiker's guide to G-quadruplex ligands. *Org. Biomol. Chem. 6*, 627–636.
20. Ou, T., Lu, Y., Tan, J., Huang, Z., Wong, K., and Gu, L. (2008) G-Quadruplexes: Targets in anticancer drug design. *ChemMedChem 3*, 690–713.
21. Read, M. A., Wood, A. A., Harrison, J. R., Gowan, S. M., Kelland, L. R., Dosanjh, H. S., and Neidle, S. (1999) Molecular modeling studies on G-quadruplex complexes of telomerase inhibitors: Structure-activity relationships. *J. Med. Chem. 42*, 4538–4546.
22. Read, M., Harrison, R. J., Romagnoli, B., Tanious, F. A., Gowan, S. H., Reszka, A. P., Wilson, W. D., Kelland, L. R., and Neidle, S. (2001) Structure-based design of selective and potent G quadruplex-mediated telomerase inhibitors. *Proc. Natl. Acad. Sci. U.S.A. 98*, 4844–4849.
23. Moore, M. J., Schultes, C. M., Cuesta, J., Cuenca, F., Gunaratnam, M., Tanious, F. A., Wilson, W. D., and Neidle, S. (2006) Trisubstituted acridines as G-quadruplex telomere targeting agents. Effects of extensions of the 3,6- and 9-side chains on quadruplex binding, telomerase activity, and cell proliferation. *J. Med. Chem. 49*, 582–599.
24. Campbell, N. H., Parkinson, G. N., Reszka, A. P., and Neidle, S. (2008) Structural basis of DNA quadruplex recognition by an acridine drug. *J. Am. Chem. Soc. 130*, 6722–6724.
25. Parkinson, G. N., Lee, M. P. H., and Neidle, S. (2002) Crystal structure of parallel quadruplexes from human telomeric DNA. *Nature 417*, 876–880.
26. Haider, S., Parkinson, G. N., and Neidle, S. (2002) Crystal structure of the potassium form of an *Oxytricha nova* G-quadruplex. *J. Mol. Biol. 320*, 189–200.
27. Haider, S. M., Parkinson, G. N., and Neidle, S. (2003) Structure of a G-quadruplex-ligand complex. *J. Mol. Biol. 326*, 117–125.
28. Fedoroff, O. Y., Salazar, M., Han, H., Chemeris, V. V., Kerwin, S. M., and Hurley, L. H. (1998) NMR-based model of a telomerase-inhibiting compound bound to G-quadruplex DNA. *Biochemistry 37*, 12367–12374.
29. Gavathiotis, E., Heald, R. A., Stevens, M. F., and Searle, M. S. (2003) Drug recognition and stabilisation of the parallel-stranded DNA quadruplex d(TTAGGGT)$_4$ containing the human telomeric repeat. *J. Mol. Biol. 334*, 25–36.
30. Parkinson, G. N., Ghosh, R., and Neidle, S. (2007) Structural basis for binding of porphyrin to human telomeres. *Biochemistry 46*, 2390–2397.
31. Parkinson, G. N., Cuenca, F., and Neidle, S. (2008) Topology conservation and loop flexibility in quadruplex-drug recognition: Crystal structures of inter- and intramolecular telomeric DNA quadruplex-drug complexes. *J. Mol. Biol. 381*, 1145–1156.
32. Dash, J., Shirude, P. S., Hsu, S. T., and Balasubramanian, S. (2008) Diarylethynyl amides that recognize the parallel conformation of genomic promoter DNA G-quadruplexes. *J. Am. Chem. Soc. 130*, 15950–15956.
33. Harrison, R. J., Gowan, S. M., Kelland, L. R., and Neidle, S. (1999) Human telomerase inhibition by substituted acridine derivatives. *Bioorg. Med. Chem. Lett. 9*, 2463–2468.
34. Storoni, L. C., McCoy, A. J., and Read, R. J. (2004) Likelihood-enhanced fast rotation functions. *Acta Crystallogr. D60*, 432–438.
35. Collaborative Computational Project No. 4 (1995) The CCP4 suite: Programs for protein crystallography. *Acta Crystallogr. D50*, 760–763.
36. Murshudov, G. N., Vagin, A. A., and Dodson, E. J. (1997) Refinement of macromolecular structures by the maximum-likelihood method. *Acta Crystallogr. D53*, 240–255.
37. Hazel, P., Huppert, J., Balasubramanian, S., and Neidle, S. (2004) Loop-length-dependent folding of G-quadruplexes. *J. Am. Chem. Soc. 126*, 16405–16415.
38. Risitano, A., and Fox, K. R. (2004) Influence of loop size on the stability of intramolecular DNA quadruplexes. *Nucleic Acids Res. 32*, 2598–2606.
39. Bugaut, A., and Balasubramanian, S. (2008) A sequence-independent study of the influence of short loop lengths on the stability and topology of intramolecular DNA G-quadruplexes. *Biochemistry 47*, 689–697.
40. Phan, A. T., Luu, K. N., and Patel, D. J. (2006) Different loop arrangements of intramolecular human telomeric (3 + 1) G-quadruplexes in K^+ solution. *Nucleic Acids Res. 34*, 5715–5719.
41. Phan, A. T., Kuryavyi, V., Luu, K. N., and Patel, D. J. (2007) Structure of two intramolecular G-quadruplexes formed by natural human telomere sequences in K^+ solution. *Nucleic Acids Res. 35*, 6517–6525.
42. Ambrus, A., Chen, D., Dai, J., Bialis, T., Jones, R. A., and Yang, D. (2006) Human telomeric sequence forms a hybrid-type intramolecular G-quadruplex structure with mixed parallel/antiparallel strands in potassium solution. *Nucleic Acids Res. 34*, 2723–2735.
43. Dai, J., Carver, M., Punchihewa, C., Jones, R. A., and Yang, D. (2007) Structure of the hybrid-2 type intramolecular human telomeric G-quadruplex in K^+ solution: Insights into structure polymorphism of the human telomeric sequence. *Nucleic Acids Res. 35*, 4927–4740.
44. Cogoi, S., and Xodo, L. E. (2006) G-quadruplex formation within the promoter of the KRAS proto-oncogene and its effect on transcription. *Nucleic Acids Res. 34*, 2536–2549.
45. Qin, Y., and Hurley, L. H. (2008) Structures, folding patterns, and functions of intramolecular DNA G-quadruplexes found in eukaryotic promoter regions. *Biochimie 90*, 1149–1171.

BI802233V